TETRAHEDRAL MESH GENERATION FOR THE STUDY OF HEAT CONDUCTION IN COMPOSITES WITH ALIGNED SHORT FIBERS OF VARIABLE ORIENTATION

Carlos F. Matt – cftmatt@lttc.coppe.ufrj.br
Universidade Federal do Rio de Janeiro, EE/COPPE/UFRJ, Departamento de Engenharia Mecânica, Cx. P. 68503 - 21945-970, Rio de Janeiro, RJ, Brasil.
Manuel E. Cruz – manuel@serv.com.ufrj.br
Universidade Federal do Rio de Janeiro, EE/COPPE/UFRJ, Departamento de Engenharia Mecânica, Cx. P. 68503 - 21945-970, Rio de Janeiro, RJ, Brasil.

Abstract*. The subject of heat conduction in short-fiber composites is gaining increased attention in light of many recent engineering applications. In this paper, we consider the important class of composites consisting of monodisperse solid thermally-conducting short fibers of circular cylindrical shape dispersed in a solid matrix. Specifically, the objective is to develop and implement a semi-automatic procedure to generate unstructured linear tetrahedral finite-element meshes in a periodic cell model microstructure. The cell is composed of a cubic matrix in which a short circular cylindrical fiber is placed at the center of the cube, the axis of the fiber lying in the horizontal XY-plane and forming an angle* φ *with the X-axis,* $0^o \le \varphi \le 45^o$*. The generated meshes are evaluated in terms of the quality of their tetrahedra. Future work shall use these meshes to calculate new results for the effective thermal conductivity of short-fiber composite materials.*

Keywords**:** *Mesh generation, Finite elements, Short-fiber composites, Heat conduction.*

1. INTRODUCTION

The subject of heat conduction in short-fiber composite materials is gaining increased attention in light of many recent engineering applications in several industries (Mirmira & Fletcher, 1999; Ayers & Fletcher, 1998; Furmanski, 1997). The engineering objective is to determine the effective thermal conductivity of composites in terms of their microstructure and component properties. Mirmira & Fletcher (1999) emphasize that flexible numerical treatments of heat conduction in composites, capable of accomodating necessary geometric and physical variations, are needed in order to understand and reproduce experimental results. In particular, finite-element approaches (Matt & Cruz, 2000; Matt, 1999; Cruz, 1998), which offer great geometric flexibility to handle complex composite geometries, require the generation of appropriate two- or three-dimensional meshes.

An important composite microstructure for heat transfer applications consists of monodisperse solid thermally-conducting short (chopped) fibers, or whiskers, of circular cylindrical shape dispersed in a solid matrix (Mirmira & Fletcher, 1999; Furmanski, 1997). One crucial step in the manufacturing processes of such composites is to press the components together, such that the fibers tend to align perpendicularly to the applied pressure. As a consequence, the fibers become transversely-aligned (lying on parallel planes but not parallel to each other in each plane), or they may even become longitudinally-aligned (lying on parallel planes and parallel to each other in each plane). As a first step to treating the former, more complex and realistic situation, Matt & Cruz (2000) modeled the latter situation by means of a periodic cell composed of a fiber placed at the center of a cube and along one of its horizontal principal axes. This paper presents a relevant extension of the work developed by Matt & Cruz (2000): here the axis of the fiber still lies in the *XY*-horizontal plane, but is now allowed to form a variable angle φ, $0^o \le \varphi \le 45^o$, with the *X*-axis. The fiber-to-cell volume ratio defines the (dispersed-phase) volume fraction, or concentration, of the composite. The objective of this work is to develop and implement a semi-automatic procedure to generate unstructured linear three-dimensional (tetrahedral) finite-element meshes in such periodic cell microstructure. In particular, we develop algorithms for the distribution of finite-element corner-nodes, or simply nodes, on lines and surfaces of the periodic cell; the distributed nodes are subsequently input to a third-party software, which then generates the required surface and volume meshes. The generated meshes are then evaluated in terms of the quality of their tetrahedra. Future work shall use these meshes to calculate new results for the effective thermal conductivity of short-fiber composite materials.

2. UNSTRUCTURED 3-D MESH GENERATION IN THE PERIODIC CELL

Finite-element mesh generation subdivides the physical domain of interest in a collection of non-overlapping conforming subdomains, called the elements. Here, as illustrated in Fig. 1, the domain is the periodic cell composed of a cubic matrix and a short fiber placed in the horizontal *XY*-plane and at the center of the cube, the axis of the fiber forming an angle φ with the *X*-axis.

Similarly to the development in Matt & Cruz (2000), the semi-automatic procedure to generate unstructured linear tetrahedral meshes in the entire volume of the periodic cell consists in six steps: first, nodes are distributed on lines and surfaces of the cell; second and third, surface meshes on the six faces of the cube and on the entire cylindrical surface of the fiber are generated; fourth and fifth, the volume meshes in the fiber and in the region between the cube and the fiber are constructed; finally, the union of these two volume meshes is effected. To generate the surface and volume meshes, we employ a third-party advancing-front generator, NETGEN (Schöberl, 1998; Schöberl, 1997), licensed to the authors for academic use.

2.1 Generation of the surface mesh on the cube

We first need to construct a *periodic* surface mesh on all six faces of the cube of side λ containing a fiber of diameter *d*, length *L*, and whose axis forms an angle φ with the *X*-axis, $0^o \le \varphi \le 45^o$ (Fig. 1). The concentration, *c*, and the aspect ratio, ρ, are nondimensional geometric parameters defined as

$$c = \frac{\pi d^2 L}{4\lambda^3}, \quad \rho = \frac{d}{L}. \tag{1}$$

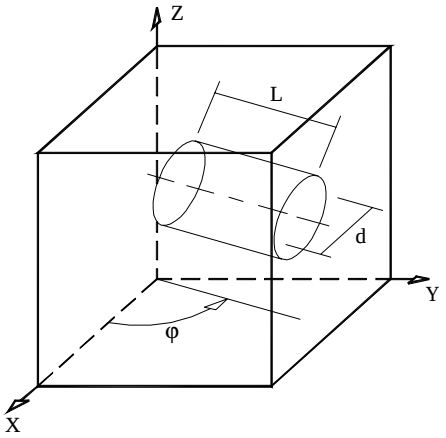

Figure 1 - Geometry of the periodic cell microstructure and associated *XYZ* Cartesian coordinate system.

The procedure to generate the desired surface mesh relies on the use of template faces, or base-faces, and consists of four essential tasks: *periodic* distribution of nodes on the four straight edges of each of three base-faces of the cube; distribution of nodes on the internal contours of the three base-faces; generation of the triangular finite-element mesh inside each base-face; and, last, appropriate translation of the three base-faces in order to construct the other three faces of the cube.

Base-face *A*, illustrated in Fig. 2(a), is a square of side λ containing a rectangle of sides *d* and *L*, whose geometric center coincides with the center of the base-face, and whose *L*-side forms an angle φ with the *X*-axis. Base-face *B*, illustrated in Fig. 2(b), is a square of side λ containing a rectangle of sides *d* and $L\cos\varphi$, whose geometric center coincides with the center of the base-face; base-face *C*, illustrated in Fig. 2(c), is similar to *B*, and contains a rectangle of sides *d* and $L\sin\varphi$. The regions defined by the rectangles are the projections of the fiber surface on the respective base-faces. With reference to the *XYZ* Cartesian coordinate system adopted, see Fig. 1, base-faces *A*, *B* and *C* are templates for the *XY*, *XZ* and *YZ* faces of the cube, respectively.

The boundary-node distribution function for two perpendicular edges and the internal contours of the base-faces takes into account the physical distance between a boundary node $\boldsymbol{P}_j$ and the solid surface of the fiber in the periodic cell, and is given by

$$h(P_j) = \frac{1}{n_r}\left(\frac{1}{m/d_{min}(P_j) + 1/h_0}\right), \tag{2}$$

$$d_{min}(\boldsymbol{P}_j) = \frac{1}{2}\big(\lambda(1+\cos(\varphi)) + 2(C_1\cos(\varphi) + d/2 - C_2\sin(\varphi) + \\ + X_{Pj}\sin(\varphi) - Y_{Pj}\cos(\varphi))\big)\sqrt{1+(tg\,\varphi)^2}\,, \tag{3}$$

$$C_1 = \frac{\lambda}{2}\big(1-\sin(\varphi)-\cos(\varphi)\big) \quad C_2 = \frac{\lambda}{2}\big(1-\cos(\varphi)+\sin(\varphi)\big), \tag{4}$$

where $h(\boldsymbol{P}_j)$ is the actual mesh spacing between $\boldsymbol{P}_j$ and the next boundary node $\boldsymbol{P}_{j+1}$, n_r is the global mesh refinement parameter, $d_{min}(\boldsymbol{P}_j)$ is the minimum distance of the node $\boldsymbol{P}_j$ to the solid surface of the fiber, according to Eq. (3), X_{Pj} and Y_{Pj} are the *X*- and *Y*-coordinates of boundary node $\boldsymbol{P}_j$, h_0 is the input default mesh spacing, and *m* is a parameter which guarantees that at least *m* elements will exist between the node $\boldsymbol{P}_j$ and the solid surface; typically, *m* = 2 and

n_r = 1 or n_r = 2. As explained in Matt & Cruz (2000), to obtain good quality triangles (triangles whose minimum internal angles exceed 30 degrees, Batdorf *et al.* (1997)) at high concentrations or high aspect ratios (when $(\lambda - d)/2h_0 < 0.01$ or $(\lambda - d/\cos\varphi)/2h_0 < 0.01$), we must insert only one node exactly in the middle of each of the two segments that connect edges of the square to the internal contours. Periodicity of the nodes on the four straight edges of each base face is guaranteed by appropriately translating the two perpendicular edges of the corresponding square, where the boundary-node distribution function (Eq. (2)) is applied.

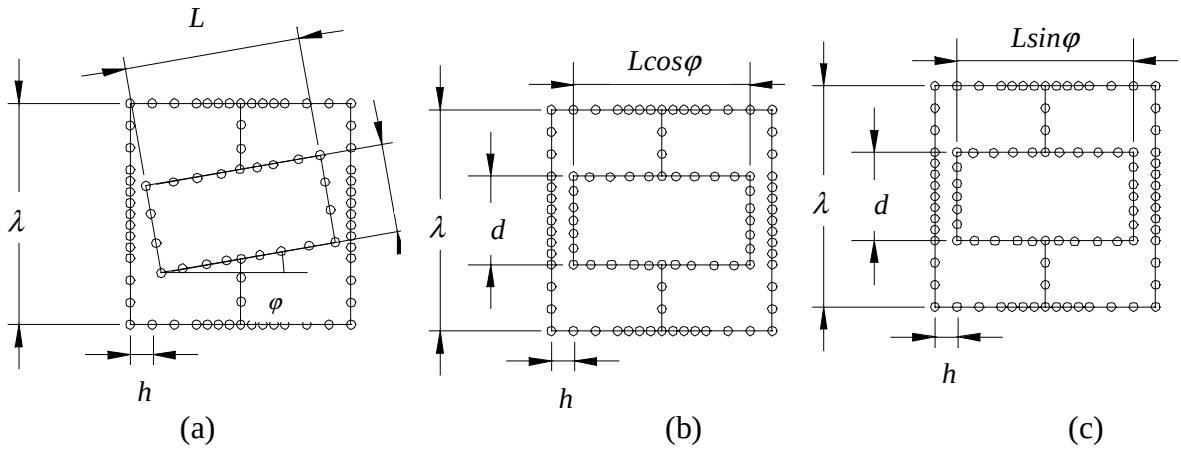

Figure 2 - Geometries of the cube base-faces *A* (a), *B* (b) and *C* (c), and respective distributions of nodes on their lines and internal contours, according to Eq. (2).

After the nodes distribution step, the coordinates and the connectivity of the distributed nodes are passed to the mesh generator NETGEN, by means of data files. The mesh generator then reads these data files, and constructs triangular (plane-surface) meshes inside the base-faces, such as the ones illustrated in Fig. 3. The periodicity of nodes around the outer edges of the base-faces can be observed. Cell periodicity is enforced by translating the base-faces *A*, *B* and *C* in the *Z*-, *Y*- and *X*-directions, respectively; therefore, opposite faces of the cube are identical. In Fig. 4, we show the periodic surface mesh on the cube obtained with the three base-faces illustrated in Fig. 3.

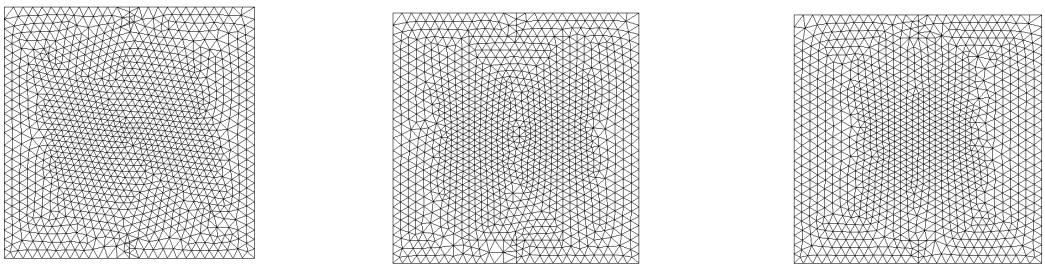

Figure 3 - Periodic triangular meshes within the cube base-faces *A* (left), *B* (center) and *C* (right); h_0/λ = 0.05, m = 2, n_r = 1, c = 0.30, ρ = 2.0, $\varphi = 20^o$.

2.2 Generation of the surface mesh on the fiber

The procedure developed to construct the surface mesh on the fiber encompasses three essential tasks: selection of primitive solids to generate the geometry of the 3-D surface to be meshed; distribution of nodes on regions of the surface to be refined; and generation of the triangular finite-element mesh on the surface of the fiber. NETGEN performs the first and

third tasks, while the user performs the second, creating a file containing the geometric data of the regions to be locally refined.

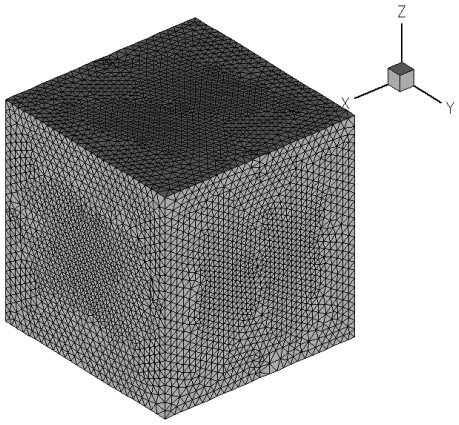

Figure 4 - Periodic cube surface mesh obtained with the three base-faces of Fig. 3; $h_0/\lambda = 0.05$, $m = 2$, $n_r = 1$, $c = 0.30$, $\rho = 2.0$, $\varphi = 20^o$.

As described in Matt & Cruz (2000), NETGEN has five primitive solids available to the user: plane, sphere, infinite length cylinder, cone, and tube. We utilize the infinite length cylinder and the plane to generate the geometry of the fiber surface. The infinite cylinder is specified through the coordinates of two points on its axis and the radius, $d/2$. The fiber is then specified by means of the intersection operation of the infinite cylinder with two parallel planes normal to the fiber axis, separated by a distance equal to L. The regions of refinement are the portions of the fiber surface closer to the other neighboring fibers; these regions are delimited by lines of nodes placed on the lateral surface and on the bases of the fiber, as illustrated, respectively, in Figs. 5(a) and 5(b). The algorithm for the distribution of nodes which define the mesh spacing $h(\boldsymbol{P}_j)$ along the boundaries of such regions is also based on Eq. (2), but now with d_{min} representing the smallest distance between a node on the fiber surface and the surfaces of neighboring fibers. A data file is then written containing the information on the primitive solids, the (X,Y,Z) coordinates of the nodes distributed on the lines of the regions of refinement, and the mesh spacing $h(\boldsymbol{P}_j)$ around these nodes. Finally, NETGEN accomplishes the third task by reading the data file and subsequently generating a non-uniform triangular finite-element mesh on the surface of the fiber, as illustrated in Fig. 6(a). During execution, NETGEN prompts the user for the value of the default spacing of the surface mesh, h_0 (entered h_0/λ) in our case.

2.3 Generation of the cell volume mesh

Subsequent to the generation of the surface meshes on the fiber and on the cube, the next step is to generate a single mesh in the entire volume of the periodic cell. To accomplish this, similarly to the description in Matt & Cruz (2000), we first generate two volume meshes, one inside the fiber and one in the region between the cube and the fiber; the union of these two volume meshes is then effected to yield the desired final mesh. These three steps are described in the paragraph below.

First, the geometric information (i.e., nodes coordinates) and the topological information (i.e., connectivity of triangles) relative to the fiber surface mesh are stored in a data file. Next, this file is read by NETGEN, which then constructs a tetrahedral volume mesh inside the fiber. Figure 6(b) illustrates the volume mesh inside the fiber, obtained from the surface mesh shown in Fig. 6(a). Second, following the generation of the periodic surface mesh on the cube

and the surface mesh on the fiber, we group all the information relative to these two meshes in a single data file. It is important to remark that, in this step, we have to invert, by node renumbering, the orientation of the triangles of the surface mesh on the fiber, relative to the orientation used to generate the volume mesh in the fiber. The data file is then processed by NETGEN in order to construct the tetrahedral volume mesh in the region between the fiber and the cube, i.e., in the matrix. Figure 7(a) illustrates the surface meshes on the cube and on the fiber surface, used by NETGEN to generate the volume mesh in the region between the fiber and the cube shown in Fig. 7(b). Third, we condense the geometric and topological information relative to the two previously generated volume meshes into one single consistent volume mesh inside the whole cell. To accomplish this, we first need to make the two volume meshes compatible at their shared boundary: we thus identify and renumber all the nodes on the fiber surface appropriately, in order to guarantee the same connectivity of nodes of the triangles shared by tetrahedra in the region between the fiber and the cube, and in the fiber. The renumbering is based on the topological, rather than on the geometric, information of the two volume meshes. Finally, the nodes of the volume mesh inside the fiber are renumbered accordingly. A conforming volume mesh inside the periodic cell, obtained from the meshes in Figs. 6(b) and 7(b), is shown in Fig. 7(c).

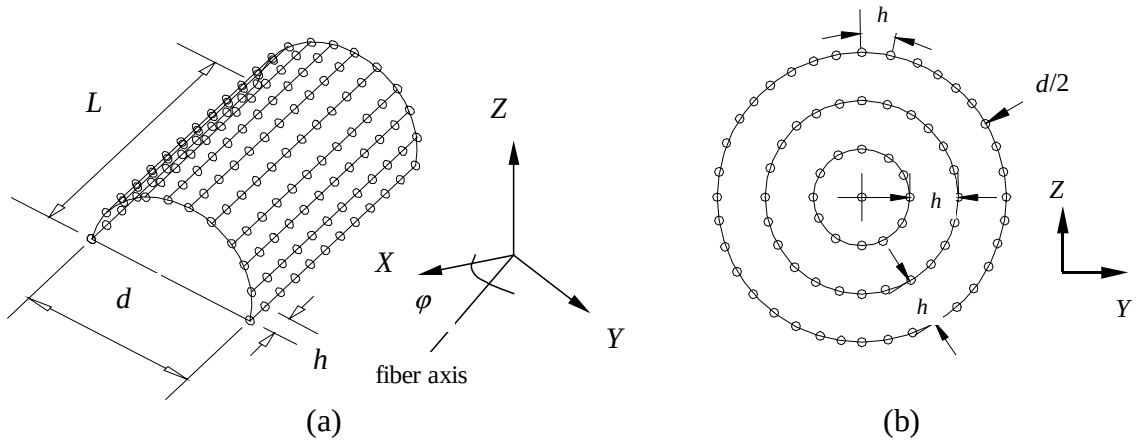

(a) (b)

Figure 5 - Nodes distributions on the lines of the regions of refinement on the lateral surface (a) and bases (b) of the fiber.

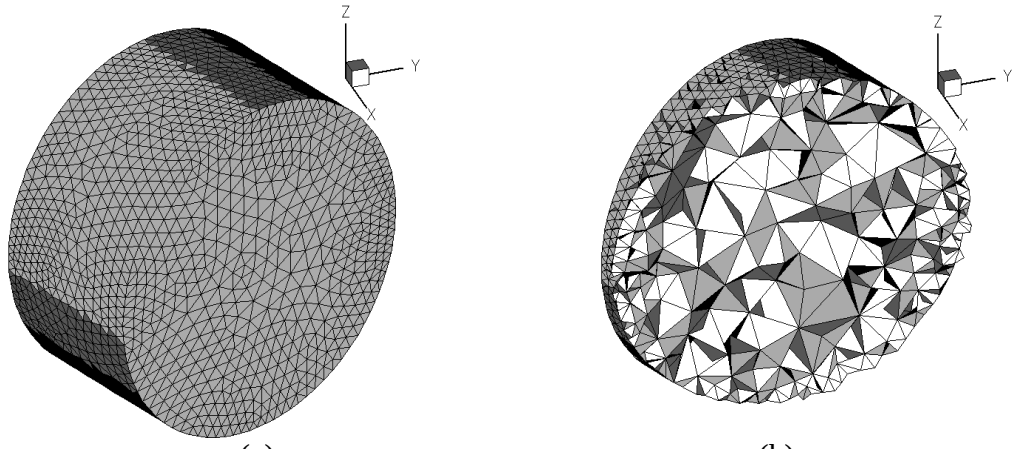

(a) (b)

Figure 6 - Surface mesh on the fiber (a) and *YZ* cross section of corresponding volume mesh inside the fiber (b); $h_0/\lambda = 0.05$, $m = 2$, $n_r = 1$, $c = 0.30$, $\rho = 2.0$, $\varphi = 20^o$.

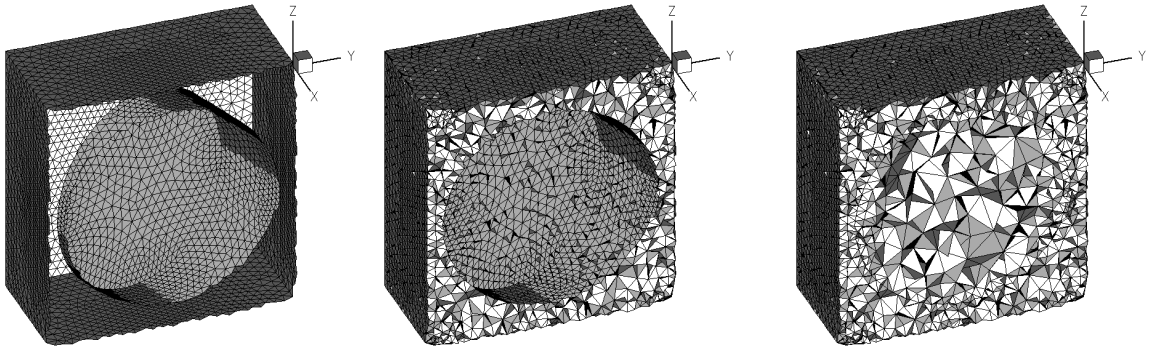

(a) (b) (c)

Figure 7 - Surface meshes on the cube and fiber (a), volume mesh in the region between the fiber and the cube (b), and *YZ* cross section of corresponding volume mesh in the periodic cell (c); $h_0/\lambda = 0.05$, $m = 2$, $n_r = 1$, $c = 0.30$, $\rho = 2.0$, $\varphi = 20^o$.

3. RESULTS AND CONCLUSIONS

In this section, we analyse several results extracted from the generation of representative tetrahedral meshes using our procedure. In Fig. 8, we show the surface meshes on fibers of eight different periodic cells with varying c, ρ and φ: $c \in \{0.10, 0.15, 0.35\}$, $\rho \in \{0.5, 2.0\}$, and $\varphi \in \{20^o, 45^o\}$. We observe that, as the concentration c increases for fixed aspect ratio ρ and fixed orientation angle φ, the meshes display the desired selective refinement in the regions where the fiber is closer to the neighboring fibers. The CPU time, in seconds, required to execute the major steps of the procedure for mesh generation inside the cells containing the fibers illustrated in Fig. 8, is shown in Table 1; the processor is a Pentium II 400 chip with 256 Mb RAM available. We observe that, in all cases, the volume meshes are considerably more time consuming than the surface meshes. Also, more CPU time is demanded to generate the volume mesh inside the matrix than inside the fiber, due to the larger volume and greater complexity of the former.

Standard tests (Dompierre *et al.*, 1998) were conducted to evaluate the quality of the tetrahedra generated by NETGEN for the eight cell volume meshes of Table 1; the results are collected in Table 2. An extremely distorted tetrahedron is rated *sliver*, and a regular or equilateral tetrahedron is rated *excellent*. In Table 2, for the eight generated cell volume meshes, the number of elements, the number of global nodes, the maximum and minimum dihedral angles, and the percentages of elements rated *sliver*, *bad*, *good* (percentage of *excellent* elements obtained by difference to 100%) are shown.

We observe in Table 2 that the presence of excessively distorted tetrahedra is small. According to the work in Matt (1999), tetrahedra rated *bad* can be kept in the mesh without affecting the accuracy and convergence of the numerical solution procedure. However, further work is needed to eliminate the tetrahedra rated *sliver*, specificallly *slivers* whose minimum dihedral angles are less than 15 degrees and/or whose maximum dihedral angles are greater than 165 degrees (Batdorf *et al.*, 1997). Batdorf *et al.* (1997) have studied the effect of unstructured finite-element mesh quality on the solution efficiency and accuracy of diffusion and advection-diffusion problems, using iterative solvers. These authors have concluded that, since it is impossible to generate a tetrahedral mesh without *slivers* from input triangular surface meshes, the dihedral angles of the mesh tetrahedra should be kept in a 'safe range'. As element angles become too small, the condition number of the element matrix sharply increases (Fried, 1972), and as element angles become too large, the discretization error in the

finite-element solution sharply increases (Babuska & Aziz, 1976). Batdorf *et al*. (1997) thus recommend the elimination of tetrahedra with dihedral angles smaller than 15 degrees and/or greater than 165 degrees. Two possible elimination strategies can be adopted. First, another 3-D mesh generator can be tested in our procedure, preferrably one that utilizes a Voronoi algorithm (Krysl & Ortiz, 1998). The second solution, slightly more complex than the first, is to devise and implement an algorithm to identify and fix the distorted tetrahedra with dihedral angles smaller than 15 degrees and/or greater than 165 degrees, by changing node coordinates; as a consequence, the mesh generated would be geometrically, but not topologically, modified (Freitag & Gooch, 1996; Joe, 1995).

As argued in Matt & Cruz (2000), the presence of tetrahedra rated *sliver* is likely to be due to the advancing front algorithms of NETGEN, which are known to not always generate elements of acceptable quality inside the domains (Krysl & Ortiz, 1998). NETGEN attempts to optimize the generated tetrahedra by performing time-consuming swapping, smoothing and splitting operations. Consequently, as can be seen in Tables 1 and 2, the CPU time is dominated not only by the number of elements (or number of global nodes), but also by the percentage of elements rated *sliver*.

The semi-automatic procedure developed here, to generate unstructured linear tetrahedral finite-element meshes for composites with aligned short fibers of variable orientation, can be used in finite-element approaches to solve the heat conduction problem in such materials, in order to determine their effective thermal conductivity. This flexible procedure permits joining many different cells together, as illustrated in Fig. 9 for two cells. Therefore, it is a basic tool for treating the more sophisticated and realistic microstructural model of transversely-aligned short fibers (Mirmira & Fletcher, 1999).

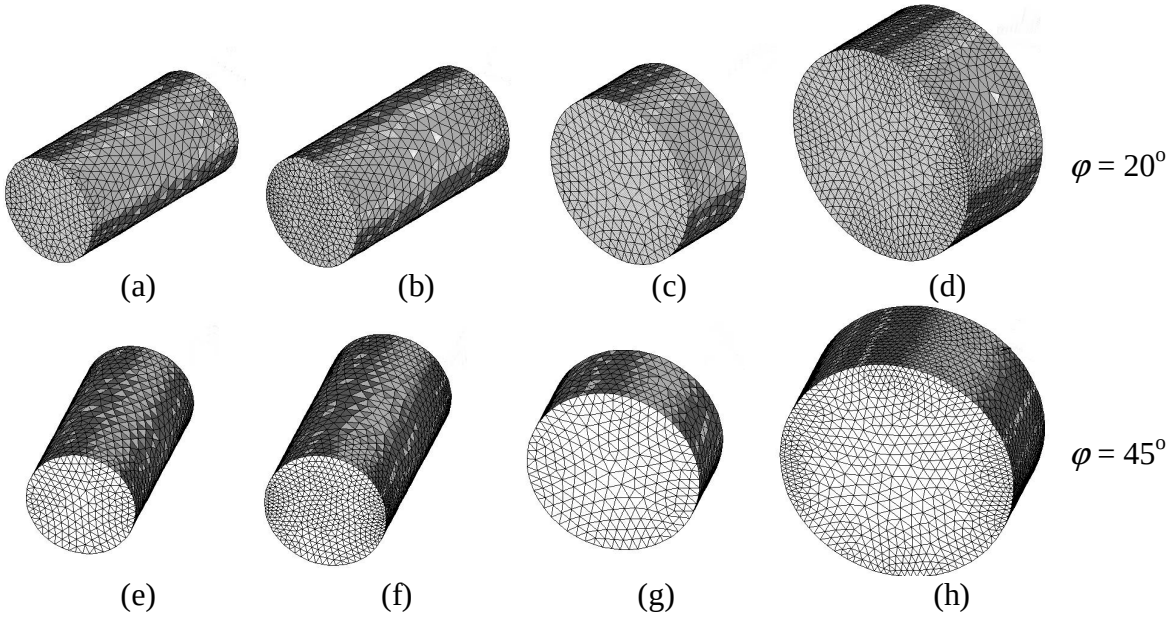

Figure 8 - Short-fibers, and corresponding surface meshes (h_0/λ = 0.05, m = 2, n_r = 1), of eight different periodic cells: (a) & (e) c = 0.10, ρ = 0.5; (b) & (f) c = 0.15, ρ = 0.5; (c) & (g) c = 0.15, ρ = 2.0; (d) & (h) c = 0.35, ρ = 2.0.

Table 1. CPU time, in seconds, required to execute the major steps of the procedure for volume mesh generation inside the periodic cells corresponding to the fibers of Fig. 8; the processor is a Pentium II 400 chip with 256 Mb RAM available

	CPU time, in seconds			
	Cube surface	Fiber surface	Fiber volume	Matrix volume
8(a)	23	6	24	1262
8(b)	25	**7**	42	778
8(c)	24	4	29	693
8(d)	26	10	77	650
8(e)	22	5	23	1328
8(f)	21	10	46	553
8(g)	25	5	31	447
8(h)	28	14	79	633

Table 2. Number of elements, number of global nodes, percentages of elements rated *sliver*, *bad*, *good*, and minimum and maximum tetrahedra dihedral angles for the eight volume meshes generated inside the periodic cells containing the fibers illustrated in Fig. 8

Evaluation tests of the quality of the tetrahedra generated by NETGEN						
	Number of elements	Number of global nodes	Sliver	Bad	Good	Min.-Max. Dihedral Angles
8(a)	89907	17709	2 %	20 %	47 %	18^o-159^o
8(b)	70754	14423	0.4 %	17.6 %	49 %	11^o-163^o
8(c)	59411	12868	1 %	24 %	46 %	8^o-162^o
8(d)	67940	15046	0.5 %	24.5 %	49 %	16^o-156^o
8(e)	94752	18555	2 %	18 %	48 %	10^o-164^o
8(f)	57185	12131	0.5 %	23.5 %	48 %	6^o-172^o
8(g)	43593	10190	1 %	31 %	45 %	12^o-158^o
8(h)	74423	16117	0.6 %	26.4 %	49 %	16^o-156^o

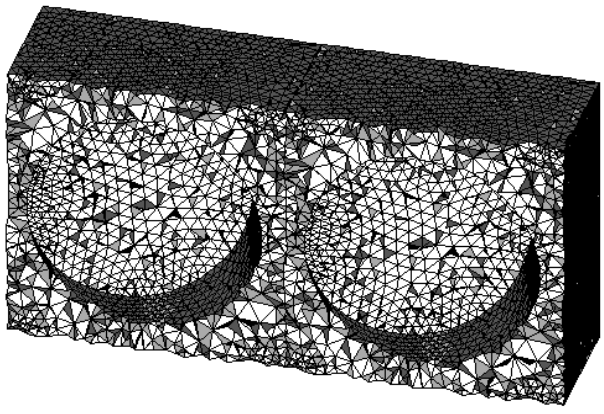

Figure 9 - Periodic cell composed of two joined (sub-)cells, where two short fibers lie in the same horizontal plane and are parallel to each other; $h_0/\lambda = 0.05$, $m = 2$, $n_r = 1$, $c = 0.30$, $\rho = 2.0$, $\varphi = 20^o$.

Acknowledgements

The authors are grateful for the support of CNPq (Grant 521002/97-4 and D.Sc. stipend of C. F. Matt) and FAPERJ. The authors also thank Prof. J. Schöberl for freely licensing NETGEN for academic use, and Mr. Daniel A. Castello for his help with some figures.

REFERENCES

Ayers, G. H. & Fletcher, L. S., 1998, Review of the Thermal Conductivity of Graphite-Reinforced Metal Matrix Composites, J. Thermophysics and Heat Transfer, vol. 12, pp. 10-16.

Babuska, I. & Aziz, A., 1976, On the angle condition in finite element method, SIAM Journal on Numerical Analysis, vol. 13, pp. 214-226.

Batdorf, M., Freitag, L. A. & Gooch, C. O., 1997, Computational Study of the Effect of Unstructured Mesh Quality on Solution Efficiency, AIAA 13th Computational Fluid Dynamics Conference, Snowmass, CO, July.

Cruz, M. E., 1998, Computation of the Effective Conductivity of Three-Dimensional Ordered Composites with a Thermally-Conducting Dispersed Phase, Proceedings of the 11th IHTC, Kyongju, Korea, vol. 7, pp. 9-14.

Dompierre, J., Labbé, P., Guibault, F. & Camarero, R., 1998, Proposal of Benchmarks for 3-D Unstructured Tetrahedral Mesh Optimization, 7th International Meshing Roundtable, Dearborn, Michigan.

Freitag, L. A. & Gooch, C. O., 1996, A Comparison of Tetrahedral Mesh Improvement Techniques, Proceedings of the 5th International Meshing Roundtable, Pittsburgh, Pennsylvania, October, pp. 87-100.

Fried, I., 1972, Condition of finite element matrices generated from nonuniform meshes, AIAA Journal, vol. 10, pp. 219-221.

Furmanski, P., 1997, Heat conduction in composites: Homogenization and macroscopic behavior, Appl. Mech. Rev., vol. 50, pp. 327-356.

Joe, B., 1995, Construction of Three-Dimensional Improved Quality Triangulations Using Local Transformations, SIAM Journal on Scientific Computing, vol. 16, pp. 1292-1307.

Krysl, P. & Ortiz, M., 1998, Generation of Tetrahedral Finite Element Meshes: Variational Delaunay Approach, 7th International Meshing Roundtable, Dearborn, Michigan.

Matt, C. F. & Cruz, M. E., 2000, Three-Dimensional Finite-Element Mesh Generation for the Study of Heat Conduction in Longitudinally-Aligned Short-Fiber Composites, Brazilian Conference on Mechanical Engineering, Natal, Brazil, to appear.

Matt, C. F. T., 1999, Heat Conduction in Tridimensional Ordered Composites with Spherical or Cylindrical Particles (in Portuguese), M.Sc. Thesis, Federal University of Rio de Janeiro, Rio de Janeiro, Brazil.

Mirmira, S. R. & Fletcher, L. S., 1999, Comparative Study of Thermal Conductivity of Graphite Fiber Organic Matrix Composites, Proceedings of the 5th ASME/JSME Joint Thermal Eng. Conference, San Diego, California, Paper AJTE99-6439, pp. 1-8.

Schöberl, J., 1997, NETGEN – An Advancing Front 2D/3D-Mesh Generator Based on Abstract Rules, Johannes Kepler Universität Linz, Institute of Mathematics.

Schöberl, J., 1998, NETGEN – User's Manual, Johannes Kepler Universität Linz, Institute of Mathematics.